

rate is of order α^{-1} while here we find a contribution which is of order α^0 . Although this contribution is small and disappears as the barrier becomes larger, it cannot be neglected as seen from the numerical results. The source of this contribution is the fact that for large values of σ the dividing surface coincides with the line $q = 0$. Along this line, in the strong-damping limit, $g' = u_1/u_{00} \gg 1$. As noted earlier, the variational surface derived from eq 2.21 is valid only as long as $g' \ll 1$. To obtain better results in the strong-damping limit, one must solve the full variational problem.

4. Discussion

Two new developments in the application of variational transition-state theory to the evaluation of reaction rates in dissipative systems have been presented in this paper. The first is a solution to the variational problem for the canonical rate based on the restriction that the dividing surface is defined only in configuration space. The result that the minimum flux is proportional to the classical action along a classical trajectory defined by a temperature-dependent Hamiltonian is the canonical version of the variational microcanonical solution.

For a 2 degrees of freedom Hamiltonian, Pechukas had shown¹⁴ that the solution to the variational problem is a classical trajectory evolving under Hamilton's equations for the same Hamiltonian. Here we find, that if one wants to take a short cut, that is, optimize the dividing surface for the canonical problem directly, then the dividing surface is again a classical trajectory, only in this case it is not limited by two equipotential lines and it evolves under the dynamics of a derived, temperature-dependent Hamiltonian. This result is quite general, applicable to any conservative 2 degrees of freedom system. Its use for dissipative systems emerges from the fact that VTST leads to the minimization of the classical flux of an effective 2 degrees of freedom Hamiltonian, as shown in refs 7 and 8. Just as in the conservative case, one can also define^{19,20} a dividing surface in the phase space of \mathbf{H}^* and optimize

such a surface. This could lead to better results than an optimization based only on a configuration space dividing surface. In other words, just as in the conservative case, the present improved variational result is not yet necessarily the best possible dividing surface.

The second part of this paper presents an application of VTST to the dissipative cubic oscillator. The major conclusion we find is that for all practical purposes, as long as the friction is ohmic and the barrier not too low, deviations from Kramers' original solution will be negligible. Previously, we reached the same conclusion for a double-well system described by a quartic potential.⁷ In the quartic case, it is sufficient to use the straight line dividing surface $\rho = 0$. In the cubic case it is necessary to use a curved dividing surface, and as a result the problem is more difficult to solve. In the quartic case, we did find though, that for memory friction, large deviations from the Grote-Hynes result are possible. It remains to apply VTST to the cubic potential in the presence of memory.

The present analysis of the cubic potential is valid only in the weak- and moderate-damping regimes of the ohmic dissipation. In the strong-damping limit, the use of the simple (quadratic) dividing surface fails and VTST gives bounds which are much larger than the Kramers result, which is exact in this limit. In the strong-damping limit one must use the numerical solution for the variational dividing surface. It remains to be seen whether the exact variational solution will lead to the correct Smoluchowski limit.

Only the spatial diffusion limit has been considered in this paper. Elsewhere we have shown¹⁹ that VTST can also be applied to the energy diffusion limit by defining a dividing surface in phase space. However, for the cubic potential, the same divergence appearing in the spatial diffusion limit appears also in the energy diffusion limit. This means that in the energy diffusion limit it is necessary to define the boundary of the energy surface, with the aid of the spatial surface derived in this paper. Application of VTST to the cubic potential in the energy diffusion limit is a topic for future work.

Acknowledgment. This work has been supported by grants from the U.S. Israel BSF and the Minerva Foundation.

(18) Van Kampen, N. G. *Phys. Rep.* **1985**, *124*, 69.

(19) Pollak, E. *Mod. Phys. Lett. B* **1991**, *5*, 13.

(20) Tucker, S. C.; Pollak, E. Submitted for publication in *J. Stat. Phys.*

Laser Flash Photolysis and Product Studies of the Photoionization of *N*-Methylacridan in Aqueous Solution

Deepak Shukla,¹ Francis de Rege,¹ Peter Wan,^{*1} and Linda J. Johnston^{*2}

Department of Chemistry, University of Victoria, Victoria, British Columbia, Canada V8W 3P6, and Steacie Institute for Molecular Sciences, National Research Council of Canada, Ottawa, Ontario, Canada K1A 0R6 (Received: February 26, 1991)

Photolysis of *N*-methylacridan (**1**) in deaerated aqueous CH_3CN solution results in photoionization, to give the *N*-methylacridan radical cation ($\mathbf{1}^{+\bullet}$) as the first-formed intermediate. Subsequent deprotonation from $\mathbf{1}^{+\bullet}$ gives *N*-methylacridyl ($\mathbf{1}^*$), which dimerizes to give 9,9'-bis(*N*-methylacridyl) (**2**) as the only isolable product. Quantum yields for loss of **1** are 0.085 and 0.022 in 1:1 $\text{H}_2\text{O}-\text{CH}_3\text{CN}$ and 100% CH_3CN , respectively. In the presence of oxygen, $\mathbf{1}^*$ is believed to be oxidized further (electron transfer to O_2), to give *N*-methylacridinium ion (**4**), which was detected by its characteristic UV absorption and fluorescence emission spectra. Laser flash photolysis studies provide direct evidence for photoionization of **1** to give the radical cation $\mathbf{1}^{+\bullet}$ which subsequently deprotonates to form $\mathbf{1}^*$. The combined transient and product studies indicate a monophotonic mechanism from the first excited state. The results demonstrate that photoexcited **1** is an excellent electron donor to bulk solvent. The process does not require externally added electron acceptors for photoredox chemistry.

Introduction

There is continuing interest in the chemistry of *N*-methylacridan (AcrH_2 , **1**) and other 1,4-dihydropyridines as model systems for

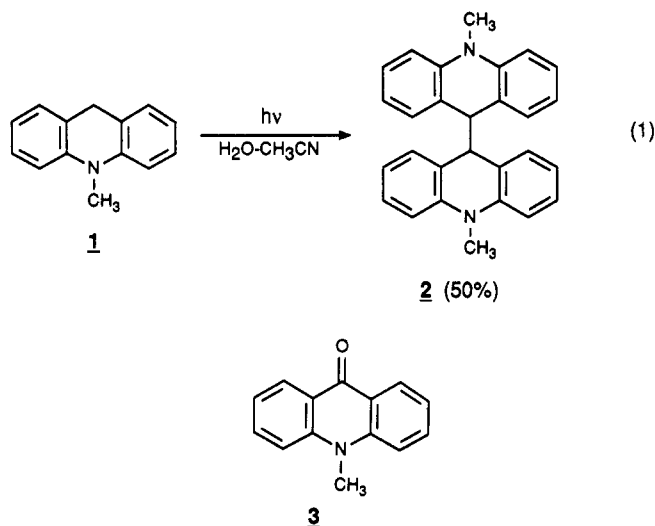
studying the redox processes involved in in vivo NADH and NADPH chemistry.^{3,4} Extensive studies by Fukuzumi and co-

(1) University of Victoria.

(2) National Research Council. Issued as NRCC 32826.

(3) Fukuzumi, S.; Tanaka, T. In *Photoinduced Electron Transfer*; Fox, M. A., Channon, M., Eds.; Elsevier: Amsterdam, 1988; Part C.

workers^{4a-c,e-i,n-q} and others^{3,4d,j-m} have shown that *N*-methylacridan (**1**) is a modest reducing agent, in both ground and excited states. For example, photolysis of AcrH₂ (**1**) in the presence of phenacyl bromide resulted in formation of *N*-methylacridinium bromide and acetophenone via an overall redox process initiated by light.^{4a} This same reaction could be sensitized with [Ru(bpy)₃]²⁺ by irradiation at 452 nm, where **1** does not absorb.^{4a} Use of photoexcited benzophenone with ground state **1** has been reported by Peters et al.⁵ to result in electron transfer from **1** to triplet benzophenone, to generate the corresponding radical anion/radical cation pair, which subsequently collapses to the radical pair after proton transfer from **1**^{•+} to benzophenone radical anion. In all of these studies, AcrH₂ (**1**) has been used for redox or photoredox chemistry in conjunction with an electron acceptor of some kind. In this work, we report that photolysis of **1** in deaerated aqueous CH₃CN solution, without any added electron acceptor molecules, results in electron ejection to bulk solvent, to give **1**^{•+}, which can be characterized spectroscopically by its transient absorption. The only isolable product from the photolysis is 9,9'-bis(*N*-methylacridyl) (**2**), which is the expected radical coupling product of **1**[•], which is formed from **1**^{•+} via loss of a proton. The results of this study may alter the mechanistic interpretations previously proposed for the photoredox chemistry of **1**, in light of the fact that photoexcited **1** will undergo electron ejection to solvents such as CH₃CN or aqueous CH₃CN without added organic electron acceptors.



Results and Discussion

Product Studies. *N*-Methylacridan (AcrH₂, **1**) was prepared from the NaBH₄ reduction of *N*-methylacridinium iodide, adapted from the procedures of Roberts et al.^{6a} and Colter et al.^{6b} The

(4) (a) Fukuzumi, S.; Mochizuki, S.; Tanaka, T. *J. Phys. Chem.* **1990**, *94*, 722. (b) Fukuzumi, S.; Mochizuki, S.; Tanaka, T. *Chem. Lett.* **1988**, 1983. (c) Fukuzumi, S.; Ishikawa, M.; Tanaka, T. *J. Chem. Soc., Perkin Trans. 2* **1989**, 1037. (d) Kano, K.; Zhou, B.; Hashimoto, S. *Bull. Chem. Soc. Jpn.* **1987**, *60*, 1041. (e) Fukuzumi, S.; Mochizuki, S.; Tanaka, T. *J. Am. Chem. Soc.* **1989**, *111*, 1497. (f) Ishikawa, M.; Fukuzumi, S.; Goto, T.; Tanaka, T. *Bull. Chem. Soc. Jpn.* **1989**, *62*, 3754. (g) Fukuzumi, S.; Kitano, T.; Mochida, K. *J. Am. Chem. Soc.* **1990**, *112*, 3246. (h) Fukuzumi, S.; Kitano, T.; Ishikawa, K. *J. Am. Chem. Soc.* **1990**, *112*, 5631. (i) Fukuzumi, S.; Kitano, T. *Chem. Lett.* **1990**, 1275. (j) Kreevoy, M. M.; Kotchevar, A. T. *J. Am. Chem. Soc.* **1990**, *112*, 3579. (k) Anne, A.; Moiroux, J. *J. Org. Chem.* **1990**, *55*, 4608. (l) Hapiot, P.; Moiroux, J.; Savéant, J.-M. *J. Am. Chem. Soc.* **1990**, *112*, 1337. (m) Schanze, K. S.; Giannotti, C.; Whitten, D. G. *J. Am. Chem. Soc.* **1983**, *105*, 6326. (n) Ishikawa, M.; Fukuzumi, S. *J. Am. Chem. Soc.* **1990**, *112*, 8864. (o) Fukuzumi, S.; Mochizuki, S.; Tanaka, T. *J. Chem. Soc., Dalton Trans.* **1990**, 695. (p) Fukuzumi, S.; Koumitsu, S.; Hironaka, K.; Tanaka, T. *J. Am. Chem. Soc.* **1987**, *109*, 305. (q) Fukuzumi, S.; Chiba, M.; Ishikawa, M.; Ishikawa, K.; Tanaka, T. *J. Chem. Soc., Perkin Trans. 2* **1989**, 1417.

(5) (a) Peters, K. S.; Pang, E.; Rudzki, J. *J. Am. Chem. Soc.* **1982**, *104*, 5535. (b) Manring, L. E.; Peters, K. S. *J. Am. Chem. Soc.* **1983**, *105*, 5708. (c) Manring, L. E.; Peters, K. S. *J. Am. Chem. Soc.* **1985**, *107*, 6452.

(6) (a) Roberts, R. M. G.; Ostović, D.; Kreevoy, M. M. *Faraday Discuss. Chem. Soc.* **1982**, *74*, 257. (b) Colter, A. K.; Saito, G.; Sharom, F. *J. Can. J. Chem.* **1977**, *55*, 2741.

TABLE I: Yields of Products from Photolysis of **1 under Various Conditions with $\lambda_{ex} = 300 \text{ nm}^a$**

solvent	product (yield)
100% CH ₃ CN (Ar purged)	<i>N</i> -methylacridone (3) ($\approx 55\%$) ^b
1:1 H ₂ O-CH ₃ CN (O ₂ purged)	<i>N</i> -methylacridinium ion ^c (4)
1:1 H ₂ O-CH ₃ CN (Ar purged)	9,9'-bis(<i>N</i> -methylacridyl) (2) ($\approx 50\%$) ^{b,d}

^a Unless otherwise indicated, conditions were as follows: 100 mg of **1** in 200-mL total volume of solvent irradiated at 300 nm for 30 min. ^b Product identified by comparison with authentic samples, by ¹H NMR. Yield calculated by integration of appropriate peaks. ^c Detected by its UV-vis absorption spectrum by comparison to an authentic sample. Yield not quantified but is the only product observed under these conditions ($\Phi = 0.022 \pm 0.004$ using 10^{-3} M of **1** with $\lambda_{ex} = 302$ nm; oxygenated 1:1 H₂O-CH₃CN solution; steady-state irradiation). ¹H NMR analysis of the product mixture after extraction with CH₂Cl₂ showed no trace of **2**. ^d Precipitate (which was shown to be product **2**) formed very early in photolysis, which blocks out irradiating light. Hence this sample was photolyzed for 120 min.

TABLE II: Yields of **2 on Photolysis of AcrH₂ (**1**) under Argon in Various Solvents^a**

solvent	% yield of 2 ^b	solvent	% yield of 2 ^b
100% hexane	5 \pm 2	100% CH ₃ CN	9 \pm 2
100% Et ₂ O	4 \pm 2	1:1 H ₂ O-CH ₃ CN	18 \pm 3
95% EtOH	9 \pm 2		

^a Photolysis conditions were 50 mg of **1** in 100-mL total volume of solvent and irradiated for 15 min at 300 nm. The optical density at 254 nm was >3 for all samples. ^b Due to the fact that **2** has very long retention times on GC columns, yields were calculated by ¹H NMR integration of the product mixture after workup. The observed conversion ratios remain similar on higher conversions.

crude white crystalline material was recrystallized several times from 95% EtOH until GC analysis showed no detectable traces of impurities.

Initial photolyses were carried out using 10^{-3} M solutions of **1** in 1:1 H₂O-CH₃CN with 254-nm lamps (Rayonet RPR 100 photochemical reactor; argon-purged and cooled solutions; 10–60 min). Prolonged photolysis yielded only a trace ($<5\%$) of 9,9'-bis(*N*-methylacridyl) (**2**), as detected by ¹H NMR of the product mixture; the rest was unreacted **1**. The solution after photolysis was a deep orange color. Remarkably, when 300-nm lamps were used, photolysis of the above solution for the same length of time resulted in efficient formation of an off-white precipitate. Analysis of the ¹H NMR spectrum of the product mixture showed ca. 50% yield of **2** (by NMR integration), along with unreacted **1** (eq 1). The pronounced change in yield of **2** by simply changing the wavelength of irradiation was not expected since organic compounds in solution generally do not have wavelength-dependent photochemistry.

Results of photolyses of **1** in the presence and absence of oxygen and/or water are shown in Table I. The products observed for the entries where oxygen was allowed into the system were identical with those already reported by Fukuzumi et al.,^{4c} who proposed a mechanism in which the primary step involves the singlet excited state of AcrH₂ (**1**) reacting with O₂ via an electron-transfer step.^{4c} However, it is clear that **1** reacts, even in the absence of oxygen, to give **2** with reasonable yields. Photolysis of **1** in H₂O-CH₃CN (argon purged) does lead to small amounts of both **3** and **4**, in addition of **2**, which was the only observable product by ¹H NMR. Both **3** and **4** have intense ($\epsilon \geq 40\,000 \text{ M}^{-1} \text{ cm}^{-1}$)^{4c} absorption maxima at ≈ 254 nm, where **1** has very little absorption (its λ_{max} is at 286 nm). Therefore, it is reasonable to propose that the observed "low" reactivity of **1** on photolysis at 254 nm is due to preferential absorption of light by traces of **3** and **4** which are formed in the photolysis. The situation is very different at 300 nm. Here, both **3** and **4** have much lower ϵ 's and **1** absorbs significantly as it is close to its λ_{max} .

Yields of **2** on photolysis at 300 nm in a variety of solvents are reported in Table II. The yields of **2** are enhanced in more polar

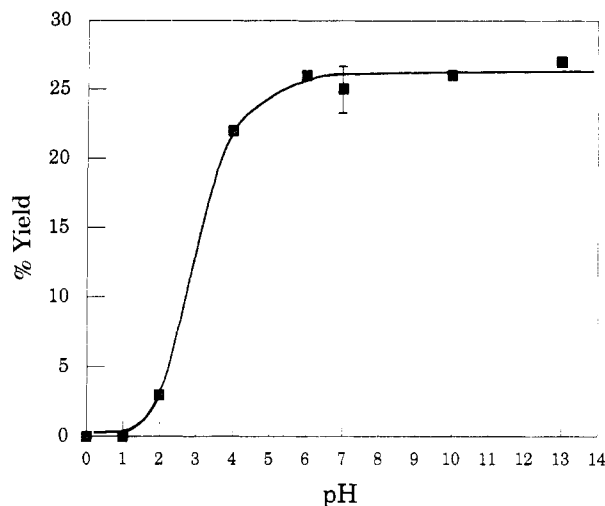


Figure 1. Plot of yield of **2** as measured by ^1H NMR integration on photolysis of **1** in 1:1 $\text{H}_2\text{O}-\text{CH}_3\text{CN}$, as a function of pH of the aqueous portion.

TABLE III: Quantum Yields for Loss of **1 (Φ_L) and Fluorescence Lifetimes in Deaerated Solvents on Photolysis at 302 nm**

solvent	Φ_L^a	τ ns ^b
100% Et_2O	0.0060	3.7 ± 0.2
100% hexane	0.0060	4.3 ± 0.2
100% CH_3CN	0.022	7.0 ± 0.2
95% EtOH	0.0080	5.6 ± 0.2
1:1 $\text{H}_2\text{O}-\text{CH}_3\text{CN}$	0.085	6.5 ± 0.2
100% H_2O^c		3.0 ± 0.2

^a Measured by GC using xanthene as external standard and potassium ferrioxalate actinometry. ^b Measured by single photon counting ($\lambda_{\text{ex}} = 300$ nm; $\lambda_{\text{em}} = 360$ nm). All decays were single exponential. ^c <2% CH_3CN cosolvent.

solvents and are especially favorable in $\text{H}_2\text{O}-\text{CH}_3\text{CN}$.

Photolyses of **1** were also carried out in 1:1 $\text{H}_2\text{O}-\text{CH}_3\text{CN}$ where the pH of the H_2O portion was changed from pH 14 to pH ≈ 0 . Yields of **2** were calculated in each experiment by integration of ^1H NMR signals and are shown in Figure 1. At pH < 2, **1** could be recovered unchanged after photolysis ruling out the possibility that a new photochemical pathway was competing at these lower pHs. The results of this study show that the protonated form of **1** is not reactive, with an apparent $\text{p}K \approx 3$. This compares favorably with a literature $\text{p}K_a$ of 3.3 reported for the ammonium ion of **1**,^{4k} which was determined in 100% CH_3CN .

Quantum Yields. Since product **2** was not readily analyzable using GC because of its long retention time and possible decomposition on the column, quantum yields for loss of substrate **1** (Φ_L) were measured instead, using xanthene as the external standard. Potassium ferrioxalate actinometry⁷ was employed at $\lambda_{\text{ex}} = 302$ nm (using the output of a 200-W Hg lamp and a monochromator with a UV band-pass filter). Because **2** was the only isolable product in these experiments, where mass balances were excellent (>90%), Φ_L (when divided by a factor of 2) should be a good measure of quantum yield for formation of **2**. Values of Φ_L are shown in Table III. The higher Φ_L in 1:1 $\text{H}_2\text{O}-\text{CH}_3\text{CN}$ compared to 100% CH_3CN , 95% EtOH, and other solvents corroborates the results of the product studies by ^1H NMR. Using the same steady-state photolysis system as described above, the quantum yield for formation of **4** in 1:1 $\text{H}_2\text{O}-\text{CH}_3\text{CN}$ was measured (monitoring at 358 nm; $\epsilon = 11800 \text{ M}^{-1} \text{ cm}^{-1}$) and gave $\Phi = 0.022 \pm 0.002$ (oxygen-purged solution) and 0.0081 ± 0.0007 (argon-purged solution).

Steady-State and Transient Fluorescence Measurements. Fluorescence spectra of **1** were taken studied using 10^{-4} M deaerated 1:1 $\text{H}_2\text{O}-\text{CH}_3\text{CN}$ solutions and excitation wavelengths

of 254 and 300 nm. Excitation at 254 nm gave an intense emission band (which increased with photolysis time) centered at 480 nm, which was identical to the emission of authentic *N*-methylacridinium ion (**4**). Two much weaker emissions were also observed centered at 425 nm (due to **3**) and at 360 nm (due to **1**). Excitation at 300 nm resulted in only the 360-nm emission, which is due to **1**. Product studies in 1:1 $\text{H}_2\text{O}-\text{CH}_3\text{CN}$ have already shown that the major product is **2**, with only trace quantities of **3** and **4**. The intense emission observed from **4** on excitation at 254 nm is due to the fact that this ion has an intense absorption at this wavelength as well as being a strongly emitting chromophore. Ketone **3** also has an intense absorption here but it is not formed to the same extent as **4** in aqueous CH_3CN solution (vide supra). Thus steady-state fluorescence measurements clearly indicate formation of both **3** and **4** on photolysis of **1** in deaerated aqueous CH_3CN . Since we have already found that **3** and **4** are the only products in oxygenated CH_3CN and aqueous CH_3CN , respectively, it is reasonable to assume that they are formed in deaerated aqueous CH_3CN because of trace amounts of oxygen present, which is difficult to remove completely from aqueous solution.

Fluorescence lifetimes were measured via single photon counting ($\lambda_{\text{ex}} = 300$ nm; $\lambda_{\text{em}} = 360$ nm) using deoxygenated solutions. Since excitation at 300 nm gave only emission from **1**, no problems from extraneous emissions were encountered. Representative lifetimes are shown in Table III. Ishikawa and Fukuzumi⁴ⁿ have reported a lifetime of 7.0 ns for **1** in 100% CH_3CN , which is in agreement with our measurement. All observed decays were single exponential. Entries from 100% CH_3CN and below indicate that a decrease in fluorescence lifetime is observed with increased Φ_L . However, both Et_2O and hexane gave lifetimes which are shorter than expected based on the measured Φ_L in these two solvents. Clearly, no simple correlation of fluorescence lifetime with efficiency of formation of product **2** exists for all the solvents used in this study. However, laser flash photolysis studies (vide infra) do show that intersystem crossing (to T_1) is more efficient in nonpolar solvents, which may offer an explanation for the shorter than expected lifetimes in these solvents. From fluorescence quenching data, Fukuzumi and co-workers^{4c} have concluded that the photoredox chemistry of **1** (in the presence of O_2) originates from S_1 .

Triplet Quenching. To our knowledge, the triplet energy of **1** has not been measured. However, it would be expected to be close to that of *N,N*-dimethylaniline and diphenylamine (E_T 's $\approx 72-75$ kcal mol^{-1}),⁸ if not lower. Use of 1,3-cyclohexadiene ($E_T \approx 53$ kcal mol^{-1})⁷ as triplet quencher would be suitable. The triplet lifetime of **1** was found to be ≥ 2 μs from laser flash photolysis experiments (vide infra). Use of a 10^{-3} M solution of triplet quencher should quench all triplet states and hence reaction to form **2** if the triplet state is indeed responsible for the observed chemistry. Photolysis ($\lambda_{\text{ex}} = 300$ nm) of a 10^{-3} M solution of **1** and a 0.003 M solution of 1,3-cyclohexadiene as triplet quencher in 100 mL of CH_3CN gave the same yield of **2** as without added quencher. This shows that the lowest triplet of **1** is not the reactive state in the photoionization process.

Laser Flash Photolysis. Laser excitation (308 nm) of deaerated samples of **1** (≈ 0.5 mM) in CH_3CN generated a strongly absorbing transient with λ_{max} at 520 nm, as shown in Figure 2. This species has a lifetime of ≈ 3 μs and reacted very efficiently with 1,3-cyclohexadiene and oxygen. For the former, a rate constant of $1.2 \times 10^{10} \text{ M}^{-1} \text{ s}^{-1}$ was determined from the slope of a plot of the observed rate constant for decay of the 520-nm signal as a function of diene concentration. These observations are consistent with the assignment of the transient to the triplet-triplet absorption of **1**. The spectrum obtained upon excitation of **1** in hexane (Figure 2) was similar to that in CH_3CN although there was somewhat less absorption in the 600-nm region. This indicated

(7) Hatchard, C. G.; Parker, C. A. *Proc. R. Soc. London, Ser. A* **1956**, *235*, 518.

(8) (a) Murov, S. L. *Handbook of Photochemistry*; Marcel Dekker: New York, 1973. (b) Carmichael, I.; Hug, G. L. In *Handbook of Organic Photochemistry*; Scaiano, J. C., Ed.; CRC Press: Boca Raton, FL, 1989; Vol. 1.

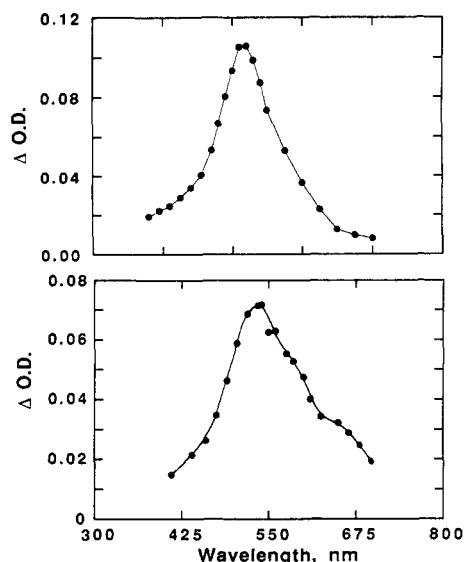


Figure 2. Transient absorption spectra produced by 308-nm excitation of **1** in hexane (top) and acetonitrile (bottom).

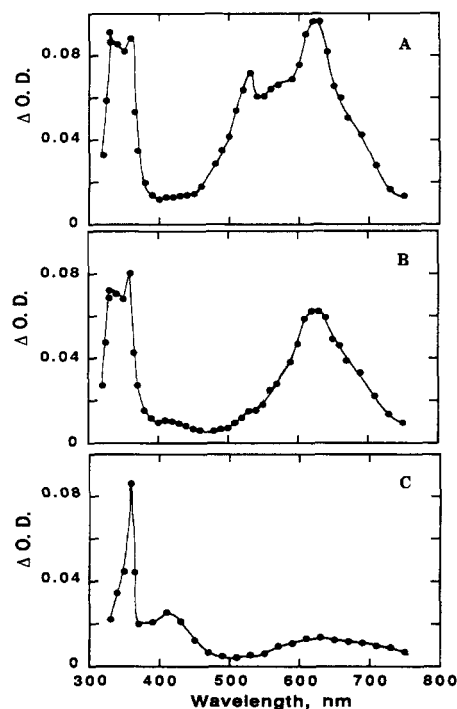


Figure 3. Transient absorption spectra measured at various delays after 308-nm excitation of **1** in 1:1 $\text{H}_2\text{O}-\text{CH}_3\text{CN}$: A, 0.5 μs ; B, 6 μs ; C, 70 μs .

that there was a small amount of another transient in addition to the triplet in CH_3CN , as did the fact the spectra recorded after most of the triplet had decayed also showed additional long-wavelength absorptions.

The origin of these longer wavelength signals was more apparent in aqueous CH_3CN . Figure 3 shows spectra recorded at three different delays after 308-nm excitation of **1** in deaerated 1:1 $\text{H}_2\text{O}-\text{CH}_3\text{CN}$ solution. The early spectrum shows a broad absorption between 600 and 700 nm and a sharper band in the 320–350-nm region. There is also a small shoulder at 520 nm, which may be attributed to triplet **1**. However, after 70 μs the long-wavelength absorption has almost completely disappeared, leaving a species with a sharp absorption at 355 nm and a weaker shoulder at ≈ 420 nm. The latter did not decay over a period of 200 μs and is readily identified as the *N*-methylacridinium ion (**4**), based on comparison of its spectrum to that of an authentic sample. Close inspection of the spectra in Figure 3 indicates that the transient with the broad absorption at long wavelengths also

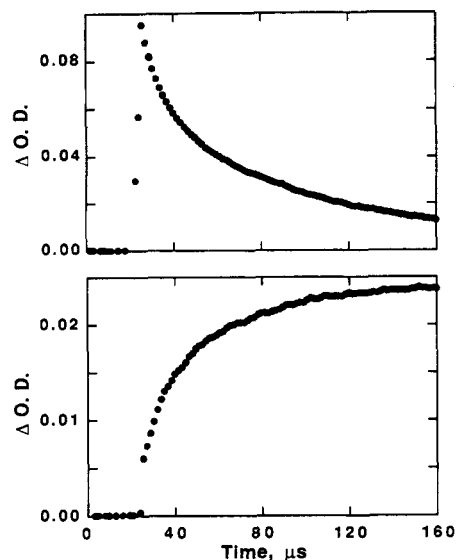


Figure 4. Plots of transient decay following 308-nm excitation of **1** in 1:1 $\text{H}_2\text{O}-\text{CH}_3\text{CN}$: top, decay of radical cation $1^{+\bullet}$ at 650 nm; bottom, growth of cation **4** at 420 nm.

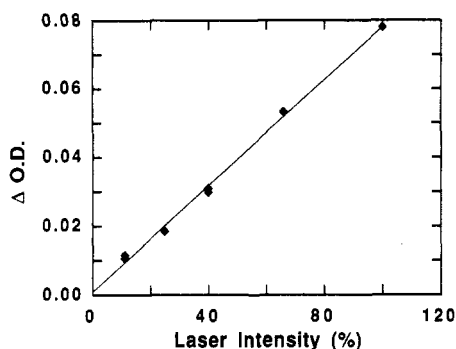


Figure 5. Plot of signal intensity due to radical cation $1^{+\bullet}$ at 650 nm in 1:1 $\text{H}_2\text{O}-\text{CH}_3\text{CN}$ as a function of the 308-nm laser intensity.

has a UV band at ≈ 330 nm. This species has a lifetime of ≈ 50 μs and is not affected by the addition of oxygen or diene. Furthermore, the spectrum is similar to that previously reported for $1^{+\bullet}$ by (i) Peters et al.⁵ for this same species and (ii) Fukuzumi et al.⁴⁰ for a charge-transfer complex between **1** and Fe^{3+} . It is also similar to the reported spectrum for the diphenylamine radical cation.⁹ The assignment of the 630-nm transient to the radical cation $1^{+\bullet}$ is further supported by its observed quenching by bases such as hydroxide or pyridine. Rate constants of 7.3×10^5 and 2×10^7 $\text{M}^{-1} \text{s}^{-1}$ were measured for reaction of the radical cation with pyridine and hydroxide ions, respectively, in 1:1 $\text{H}_2\text{O}-\text{CH}_3\text{CN}$. Note that the rate constant for pyridine is in reasonable agreement with that measured for deprotonation of $1^{+\bullet}$ in CH_3CN ($+0.6$ M tetraethylammonium tetrafluoroborate) from simulations of electrochemical data (3.1×10^6 $\text{M}^{-1} \text{s}^{-1}$)⁴¹ and by direct measurement (2×10^6 $\text{M}^{-1} \text{s}^{-1}$).^{4p} Time-resolved conductance measurements also confirmed the formation of ionic species. The yield of radical cation $1^{+\bullet}$ was similar ($\pm 20\%$) for either nitrogen- or oxygen-purged samples.

Examination of decay traces at various wavelengths indicated that the triplet and radical cation signals were formed rapidly within the duration of the laser pulse. However, the signal due to **4** at 420 nm showed a readily resolvable growth on long time scales, which agreed well with the decay of $1^{+\bullet}$ at 650 nm. Traces recorded at the two wavelengths are shown in Figure 4. Note that a small fraction of the 420-nm signal is formed rapidly. This is due to some residual absorption from the triplet at this wavelength. The growth of **4** cannot be detected at its UV maximum due to overlap with the radical cation signal in this region.

The effect of laser dose on the formation of the radical cation was examined. A plot of signal intensity as a function of laser intensity was linear over a range of laser intensities which varied by a factor of 10 (Figure 5). This suggests that the photoionization is monophotonic, although it is possible under special circumstances to obtain linear plots for biphotonic processes.¹⁰ Excitation of **1** at 266 nm in 1:1 H₂O-CH₃CN gave similar ratios of radical cation and triplet signals to those obtained using the 308-nm laser. These results are also indicative of a monophotonic process.

A two-laser experiment¹¹ in which triplet **1** was generated in aqueous CH₃CN and then reexcited ≈ 100 ns later with a 530-nm Nd:YAG laser pulse was also carried out. A small amount of bleaching of the triplet at 520 nm was observed, along with the concomitant formation of additional radical cation at 640 nm. These results demonstrate that photoionization can occur from an upper triplet state. However, the lowest energy triplet is not responsible for the observed one-laser photoionization since all the radical cation is formed within the laser pulse, whereas the triplet absorption decays over a period of several microseconds. As noted above, product studies in the presence of diene also led to the same conclusion.

Excitation of **1** in methanol gave a considerably lower yield of radical cation than did aqueous CH₃CN but a larger amount of triplet. We did not observe any absorptions in the 700-nm region which could be assigned to the solvated electron, probably as a result of the lower efficiency of photoionization in this solvent. In CH₃CN the electron is known to exist as a mixture of monomeric and dimeric radical anions which absorb weakly between 500 and 1500 nm and would not be readily detectable in our experiments.¹² Solubility problems prevented our examining the photochemistry of **1** in pure H₂O, where hydrated electrons can be readily observed between 700 and 800 nm.

The above results do not provide any evidence for the intermediacy of the *N*-methylacridyl radical (**1**[•]), which is presumably formed by deprotonation of **1**^{•+}. Previous pulse radiolysis work¹³ as well as microsecond flash excitation of the *N*-methylacridinium ion (**4**) in the presence of cuprous ion¹⁴ have demonstrated that this radical has a relatively weak absorption at 510 nm. We reasoned that the radical would be more readily detected if the radical cation lifetime was shortened by the addition of base. Accordingly spectra were recorded for a sample of **1** in 1:1 H₂O-CH₃CN containing 0.038 M sodium hydroxide. This hydroxide concentration shortens the radical cation lifetime to ≈ 1.5 μ s, which is similar to the triplet lifetime in deaerated solution. This experiment indicated that there was another species in addition to the triplet in the 500-nm region; however, it was not particularly long-lived (5–10 μ s) and it was difficult to separate it from the triplet, which absorbs strongly in the same region (Figure 2).

The above problems were overcome by repeating the same experiments in the presence of both hydroxide (to reduce the radical cation lifetime) and 0.0025 M 1,3-cyclohexadiene (to quench the triplet). The resulting spectra are shown in Figure 6. The early spectrum shows both radical cation (**1**^{•+}) and cation (**4**), as well as an additional signal at 510 nm with a shoulder at 490 nm, in good agreement with the published spectrum for the *N*-methylacridyl radical (**1**[•]).¹⁴ The latter cannot be triplet **1** since the amount of diene used is sufficient to shorten the triplet lifetime to ≈ 30 ns. The late spectrum in Figure 6 shows only **1**[•] and **4**. At even longer delays after the laser excitation, only the cation (**4**) remains.

The decay of the radical cation and radical signals as well as the growth of **4** at 420 nm was examined under a variety of

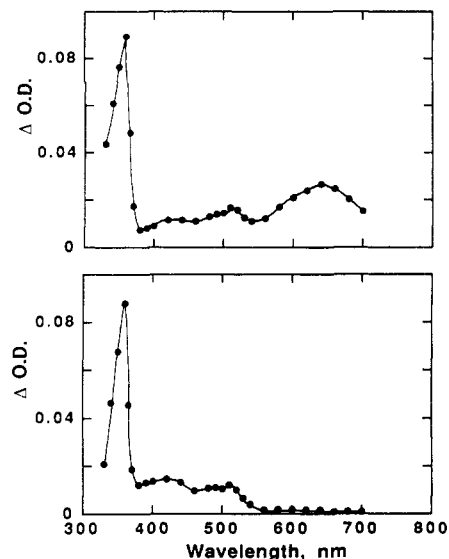


Figure 6. Transient absorption spectra measured 1 μ s (top) and 10 μ s (bottom) after 308-nm laser excitation of **1** in 1:1 H₂O-CH₃CN containing 0.025 M NaOH and 0.0025 M 1,3-cyclohexadiene.

conditions in an attempt to determine the mechanism for formation of **4**. It has already been pointed out that the kinetics for the growth of **4** agree well with those for the decay of **1**^{•+} in the absence of base (Figure 4). However, the lifetime of radical **1**[•] is substantially shorter than that of **1**^{•+} under these conditions so either **1**[•] or **1**^{•+} could be the precursor for **4**. In the presence of sufficient hydroxide and diene to allow the detection of the radical **1**[•] it is possible to show that formation of the radical is concomitant with the decay of radical cation **1**^{•+}. Further, under these conditions the growth of **4** occurs more slowly than the decay of **1**^{•+} but is in reasonable agreement with the decay of the radical monitored at either 520 or 480 nm. Addition of small amounts of air to the sample resulted in a more rapid decay of the radical and a concomitant increase in the rate for production of cation **4**. However, addition of air does not decrease the yield of **4**; similarly, either oxygen- or nitrogen-purged samples gave the same yield of **4**. These results indicate that most of cation **4** is formed from radical **1**[•], at least under these conditions.

The quantum yield of cation **4** generated by 308-nm laser excitation of **1** in 1:1 H₂O-CH₃CN was evaluated by measuring the signal intensity due to **4** at 420 nm and using a value of 3300 M⁻¹ cm⁻¹ for the extinction coefficient at this wavelength. A sample of Aberchrome-540 in toluene with matched optical density at the laser wavelength was used as the actinometer. Comparison of the signal intensity for **4** and the actinometer as a function of the laser intensity gave a value of ≈ 0.1 for the quantum yield of formation of **4**.

Mechanism of Reaction. The results presented in this study would argue for a mechanism of reaction of **1** (in the absence of oxygen) in which the primary step is photoionization from S₁ (Scheme I), to generate *N*-methylacridan radical cation (**1**^{•+}). The major reaction pathway for **1**^{•+} is deprotonation, to give the corresponding radical **1**[•]; the intermediacy of **1**[•] is demonstrated by both isolation of its dimerization product **2** in steady-state experiments and its direct detection in the transient experiments. Intersystem crossing to triplet **1** does occur but leads to no chemistry. The lifetime of radical cation **1**^{•+} is shortened in the presence of hydroxide ion, presumably due to enhancement of the deprotonation rate to form **1**[•]. However, since no overall increase in yield of **2** was observed on increasing the pH, the product-limiting step is ionization, which is probably irreversible.

Both product studies and transient results suggest that photoionization of **1** is a monophotonic process. This is somewhat unusual since a number of recent results have reported that biphotonic processes involving upper singlet or triplet states are important in a number of photoionizations.^{15–17} However, there

(10) Lachish, U.; Shafferman, A.; Stein, G. *J. Chem. Phys.* **1976**, *64*, 4205.

(11) Scaiano, J. C.; Johnston, L. J.; McGimpsey, W. G.; Weir, D. *Acc. Chem. Res.* **1988**, *21*, 22.

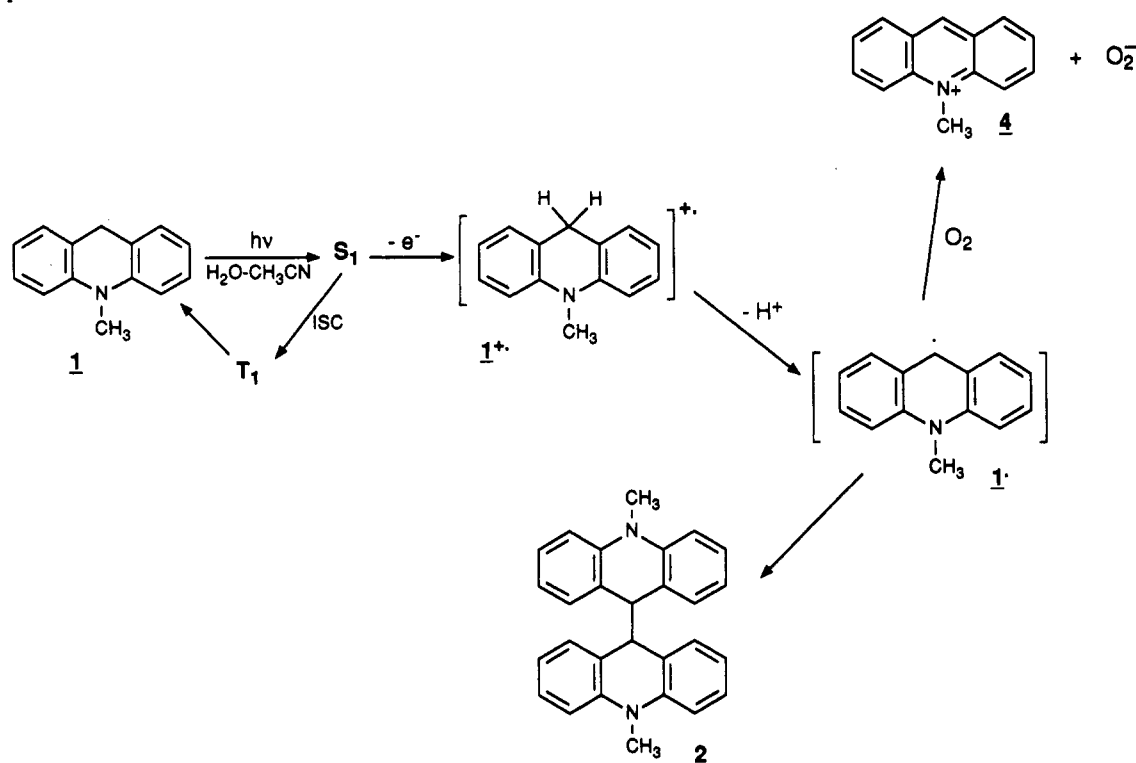
(12) Bell, I. P.; Rodgers, M. A. J. *J. Chem. Soc., Faraday Trans. 1* **1977**, *73*, 315.

(13) Neta, P. *J. Phys. Chem.* **1979**, *83*, 3096.

(14) Poulos, A. T.; Hammond, G. S.; Burton, M. E. *Photochem. Photobiol.* **1981**, *34*, 169.

(15) Steenken, S.; McClelland, R. A. *J. Am. Chem. Soc.* **1989**, *111*, 4967.

SCHEME I



are also several reports of monophotonic photoionizations of 1,3-dioxoles, unsaturated hydrocarbons, and aromatic hydrocarbons.¹⁸⁻²⁰ The observed photoionization upon excitation of triplet **1** is not surprising, given that the sum of the triplet energy and a 530-nm photon is $\approx 128 \text{ kcal mol}^{-1}$, which is well in excess of the singlet energy of **1**.

Cation **4** has been observed in both steady-state and transient experiments, although in considerably different yields (vide supra). Three possible mechanisms for its formation are (1) loss of hydrogen atom from $1^{+\bullet}$, (2) oxidation of radical 1^{\bullet} , and (3) reexcitation of either 1^{\bullet} or $1^{+\bullet}$ followed by loss of a hydrogen atom or an electron. The third possibility can be easily ruled out on the basis of the fact that **4** is not produced instantaneously. The laser experiments indicate that the majority of **4** does not come directly from the radical cation $1^{+\bullet}$, although the presence of a small contribution from such a pathway cannot be ruled out by our results. The alternate possibility (oxidation of 1^{\bullet}) is consistent with the fact that the growth of cation **4** is concomitant with the decay of 1^{\bullet} under a variety of experimental conditions. A possible mechanism is electron transfer from the radical 1^{\bullet} to oxygen, which should be energetically feasible based on redox potentials of -0.40 V^{21} for reduction of oxygen and -0.43 V^{4p} (-0.46^{4l}) for reduction of **4**. This is also consistent with the fact that reaction of oxygen with the radical does not decrease the yield of the cation. However, it does mean that the solutions used for the laser and steady-state experiments must still have sufficient oxygen for trapping of radical 1^{\bullet} by oxygen to compete with its dimerization. This is not unreasonable given the fact that nitrogen or argon purging (particularly of aqueous solutions) does not completely remove oxygen from these samples. We have already shown in product studies that when the solution is purged with oxygen, the only product is **4**. Presumably in this case, all radicals (1^{\bullet}) are trapped by oxygen to give **4**. The higher yield of cation in the laser exper-

iments compared to that from steady-state irradiation is puzzling. It may be that **4** is photolabile under steady-state (long times) irradiation, leading to an apparently lower yield. This is not an unreasonable suggestion, based on the fact that photolysis of **4** has been reported to yield dimer **2**.^{4g}

Fukuzumi and Tanaka^{4c} have studied the photolysis of **1** in aqueous CH_3CN solution in the presence of O_2 and reported that the primary step is electron transfer from photoexcited **1** to oxygen, to generate a radical cation/anion pair. Subsequent transformation of this species depended on whether the solvent was pure CH_3CN or aqueous CH_3CN with added H^+ , but in each case involving the initially formed *N*-methylacridyl radical from decomposition of the radical cation/anion pair. Our results show that the presence of oxygen is *not* a necessary condition for the formation of radical cation from photoexcited **1** in aqueous CH_3CN , since this intermediate has been directly detected in N_2 -purged samples. Although under these conditions (solutions deaerated with Ar or N_2) there was a sufficient amount of oxygen to give trace yields of oxidized photoproducts (viz., **3** and **4**), the possibility that the first (photoionization) step involves a bimolecular reaction with oxygen is unlikely since the yield of $1^{+\bullet}$ was not noticeably different in N_2 - versus O_2 -saturated solutions (vide supra). In addition, the amount of oxygen in solution in N_2 -purged samples ($< 10^{-4} \text{ M}$)^{8a} would not quench the singlet state of **1** ($\tau \leq 7.0 \text{ ns}$ from Table III) significantly, even using $k_q \approx 10^{10} \text{ M}^{-1} \text{ s}^{-1}$, which was determined by Fukuzumi et al.^{4c} Our results suggest that oxygen does react with photogenerated 1^{\bullet} , to give **4**. In N_2 - or Ar₂-purged solutions, this rate is slow and the majority of photogenerated 1^{\bullet} dimerizes to give **2** (Scheme I).

Summary. Product and laser flash photolysis studies have shown that *N*-methylacridan (AcH_2 , **1**) undergoes one-electron ionization from S_1 on photolysis in deoxygenated aqueous solution. The ionization is a one-photon process. The major pathway for reaction of photogenerated $1^{+\bullet}$ is deprotonation of one of the benzylic protons, to generate *N*-methylacridyl (1^{\bullet}), which dimerizes to give **2**. In the presence of oxygen, 1^{\bullet} is oxidized to *N*-methylacridinium ion (**4**), which is a minor pathway in deaerated solution.

Experimental Section

Materials. *N*-Methylacridan (AcH_2 , **1**) was made by $NaBH_4$ reduction of *N*-methylacridinium iodide (**4**), which was in turn

(16) Johnston, L. J.; Lobaugh, J.; Wintgens, V. *J. Phys. Chem.* **1989**, *93*, 7370.

(17) Steenken, S.; Warren, C. J.; Gilbert, B. C. *J. Chem. Soc., Perkin Trans. 2* **1990**, 335.

(18) Trampe, G.; Mattay, J.; Steenken, S. *J. Phys. Chem.* **1989**, *93*, 7157.

(19) Vauthey, E.; Haselbach, E.; Suppan, P. *Helv. Chim. Acta* **1987**, *70*, 347.

(20) Delcourt, M. O.; Rossi, M. J. *J. Phys. Chem.* **1982**, *86*, 3233.

(21) Sawyer, D. T.; Valentine, J. S. *Acc. Chem. Res.* **1981**, *14*, 393.

made via reaction of *N*-methylacridine (purchased from Aldrich) with methyl iodide, all following published procedures.^{6a,b} The material was recrystallized several times from 95% EtOH and stored in the refrigerator under argon. Fresh samples from the refrigerator were used for all studies. *N*-Methylacridone (3) and 1,3-cyclohexadiene were purchased from Aldrich, the latter was distilled before use.

Product Studies. Photolyses of 1 were carried out by using 10^{-3} M solutions in 200 mL of solvent in quartz tubes. Cooling was accomplished with an internal cold finger at ≈ 12 °C. Argon (or oxygen purge) was accomplished by using a long syringe needle inserted into the quartz vessel. The quartz tube was photolyzed in a Rayonet RPR 100 photochemical reactor (16 lamps) with 300- or 254-nm lamps. Photolyses times were controlled with a standard timer. After photolysis, the solution (along with any precipitate formed) was extracted several times with CH_2Cl_2 . After removal of the solvent, the product mixture was analyzed by ^1H NMR. Conversion to 2 was calculated from integration of peak areas of substrate and product signals. Isolated 9,9'-bis(*N*-methylacridyl) (2) (mp 238 °C) had an identical ^1H NMR spectrum with that reported in the literature.^{4g}

Fluorescence Measurements. Steady-state fluorescence spectra were recorded at ambient temperature on a Perkin-Elmer MPF 66 instrument and were not corrected for photodetector response. Fluorescence lifetime measurements were carried out using time-resolved single photon counting, on a Photon Technology International LS-1 instrument with standard photon counting electronics. All reported lifetimes were calculated from good single exponential decays. Solutions used were $\approx 10^{-5}$ M and were purged with a stream of high-purity argon (or oxygen when desired) for 5–10 min prior to measurement.

Quantum Yield Measurements. Quantum yields for loss of substrate (*N*-methylacridan (1)) were measured using the output of an Oriel 200-W Hg lamp filtered through an Applied Photo-physics monochromator set at 302 nm and a UV band-pass filter. Cuvettes containing $\approx 10^{-3}$ M substrate in the appropriate solvent (3.0 mL) were irradiated for 5–30 min after purging with a stream of argon. The solution was then extracted with CH_2Cl_2 , xanthene (external standard) was added, and the mixture was analyzed by GC. Potassium ferrioxalate actinometry⁷ was used for light intensity measurements.

Laser Flash Photolysis. Either a Lumonics EX-510 excimer laser (XeCl gas mixtures; 308 nm; 8 ns pulses; <50 mJ/pulse) or a Lumonics HY750 Nd/YAG laser (second or fourth harmonic, 535 or 266 nm; 10-ns pulses; <45 mJ/pulse at 266 nm) was used for sample excitation. Samples were contained in 7×7 mm² flow cells connected to a solution reservoir with Teflon tubing. The use of flow samples was essential to minimize problems due to the buildup of minor amounts of fluorescent products. Unless otherwise noted, the samples were deaerated by bubbling nitrogen through the solution for a least 30 min prior to laser excitation. Further details of the apparatus have been reported elsewhere.²²

Acknowledgment is made to the donors of the Petroleum Research Fund, administered by the American Chemical Society, for partial support of this research (at Victoria). Additional support was provided by the Natural Sciences and Engineering Research Council (NSERC) of Canada (at Victoria). We thank P. Wu for carrying out some preliminary experiments.

(22) Kazanis, S.; Azarani, A.; Johnston, L. J. *J. Phys. Chem.* 1991, 95, 4430.

Quantum Thermodynamics: The Microscopic Basis of Entropy and Linear Thermodynamic Relations

William Rhodes

Department of Chemistry, Institute of Molecular Biophysics, Florida State University, Tallahassee, Florida 32306 (Received: February 26, 1991; In Final Form: August 8, 1991)

Thermodynamic processes in condensed molecular systems are described here in terms of the oscillator-type thermal modes of the system. Chemical reactions generally involve thermal mode transformations, which include changes in either or both the frequency and the zero-point energy level of various thermal modes. We show that the entropy of a set of equivalent (equal frequency) thermal modes may be expressed as a sum of two terms, each having definite geometrical and physical meaning. One of the terms is the compensation entropy proposed by Benzinger to balance the thermal energy in the expression for the free energy of the system. The spectrum of thermal mode frequencies of a condensed molecular system covers a broad range of values. At ambient temperatures in most systems, elementary quantum effects result in many of the higher frequency modes being thermally inactive or "frozen". The concept of thermal mode thawing is presented as a fundamental element in thermodynamic processes, in general, and in isothermal processes, in particular. It is shown how linear thermodynamic relations within a family of reactions may result from the variation among family members in the number of thermal modes undergoing either (i) a frozen \leftrightarrow thawed transition or (ii) a mode softening concomitant with a shift of zero-point energy level. The importance of these concepts for condensed system reactions in general, and for processes in biological macromolecules in particular, is emphasized.

Introduction

The quantum theoretical basis of thermodynamics is very well established and forms the standard approach of most books on statistical mechanics. A system consisting of N atoms has $3N$ spatial degrees of freedom, in addition to any intrinsic degrees of freedom each atom might have. The $3N$ spatial degrees of freedom are divided among translational, rotational, vibrational, etc., degrees of freedom, depending on the molecular structure of the system and the cohesive nature of the intermolecular forces. Each of these degrees of freedom which is at thermal equilibrium at temperature T is referred to as a *thermal mode*. The quantum

and thermodynamic properties of each kind of thermal mode are well-known, and together such modes provide the simple models used in text books.

Furthermore, for condensed molecular systems, thermal modes characterized by harmonic oscillations are fundamental to the thermodynamics of the system as is witnessed by classic works of Kirchoff, Wien, Rayleigh, and others, in the 1800s, on equilibrium radiation density of solids extending to the quantum formulations of Planck, Einstein, and Debye in the early 1900s. The discussions of this paper concern the thermodynamic properties associated with harmonic oscillator type thermal modes of